

## Linear drift-wave instability in TJ-K geometry

M. Ramisch, G. Birkenmeier, A. Köhn, U. Stroth

*Institut für Plasmaforschung, Universität Stuttgart, Germany*

**Introduction:** For the magnetic confinement of fusion plasmas, stellarators offer a great flexibility for the optimization of plasma properties through the magnetic configuration. Present day stellarators are already optimized with respect to neoclassical transport. As suggested by stability theory, the geometrical properties of the confining magnetic field like magnetic field-line curvature and magnetic shear also affect the microscopic structure of turbulence. Hence, the optimization with respect to turbulent transport is an important issue in current research.

In the stellarator TJ-K, the plasma dynamics is governed by drift-wave turbulence [1]. Recently, experimentally observed poloidal asymmetries in the turbulent cross-field transport could be correlated with the field-line curvature in the TJ-K geometry [2]. The aim of this work is to obtain a deeper understanding of this correlation by means of calculated linear growth rates of drift-wave instabilities. To this end, a drift-fluid model is utilized and growth rates are calculated from a simple dispersion relation incorporating the geometrical quantities of the magnetic field in TJ-K. The theoretical result is compared to measured poloidal profiles of turbulent transport.

**Poloidal transport asymmetry:** The experiments were conducted in 2.45 GHz microwave heated (1.8 kW) helium discharges in the stellarator TJ-K [1] with  $\bar{n} \approx 1.4 \times 10^{17} \text{ m}^{-3}$  and  $T_e$  about 13 eV ( $T_i \lesssim 1$  eV). A 64-pin poloidal probe array measured fluctuations in the ion-saturation current ( $\tilde{I}_{i,\text{sat}} \sim \tilde{n}$ ) and the floating potential ( $\tilde{\phi}_f \sim \tilde{\phi}$ ) in alternating order at a toroidal position with triangular flux-surface shape. From the signals, the cross-field turbulent transport  $\Gamma = \langle \tilde{n} \tilde{v}_r \rangle_t$  with  $\tilde{v}_r = \tilde{E}_\theta / B = -\Delta \tilde{\phi}_f / (2\Delta y B)$  can be approximated at 32 positions in the poloidal cross section on an inner flux surface in the density gradient region. The poloidal profile of  $\Gamma$  is shown in Fig. 1 as a function of the probe position in terms of the full poloidal circumference of the flux surface.  $y = 0$  corresponds to the outboard midplane on the low-field side (LFS).

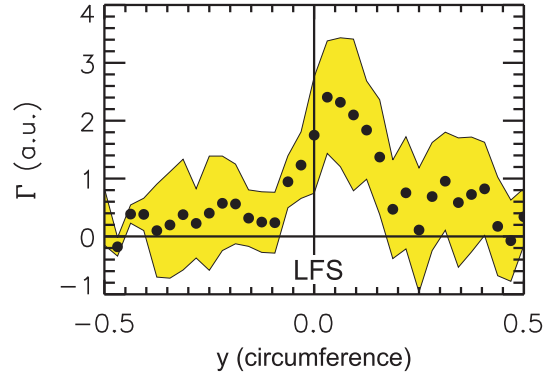


Fig. 1: Temporally averaged turbulent transport  $\Gamma$  as a function of the poloidal position (in units of the full circumference, ccw). Zero is centred on the LFS. The scatter of  $\Gamma$  is shaded.

$\Gamma$  exhibits a strong poloidal dependency with a distinct maximum on the LFS, which, in particular, can be attributed to locally enhanced deviations in the spatial  $\tilde{n}$ - $\tilde{\phi}$  phase relation from zero [3]. Magnetic field calculations showed that the transport maximum coincides with the region of negative normal curvature of the field lines. In addition, however, the maximum is found poloidally shifted into the direction of the ion-diamagnetic drift. A misalignment of the probe tips could be ruled out as a possible cause of this shift. The transport maximum was found to be rather correlated with a combination of negative normal and positive geodesic curvature [2]. The examination of theoretical linear growth rates provides some insight into this effect.

**Linear growth rates:** For an experiment-theory comparison, linear growth rates can be calculated from a drift-fluid model (see e.g. Refs. [4, 5, 6, 7, 8]). To this end, the linearised ion-continuity equation – containing terms up to first order in the drift parameter – is combined with the parallel component of the ion equation of motion  $\partial_t \tilde{n} = -\tilde{\mathbf{v}}_{E \times B} \cdot \nabla \ln n_0 - \nabla \cdot (\tilde{\mathbf{v}}_{pol} + \tilde{\mathbf{v}}_{E \times B} + \tilde{\mathbf{v}}_{\parallel})$ . The compression and decompression introduced by the inhomogeneity of the magnetic field ( $\nabla \cdot \tilde{\mathbf{v}}_{E \times B} = -2\tilde{\mathbf{v}}_{E \times B} \cdot \kappa$  with  $\kappa$  the magnetic field-line curvature) counteracts the effect of particle flux up and down the density gradient, respectively. The fluctuations in the density are related to those in the potential through the  $i$ - $\delta$  approach by a constant phase shift  $\tilde{n} = (1 - i\delta)\tilde{\phi}$ . After separation of perpendicular and parallel scales an eigenvalue problem is to be solved for the potential eigenmodes along a field line around points of interest on the flux surface (details can be found in e.g. Ref. [7]). This allows for comparisons of corresponding growth rates with geometric features of the magnetic field as curvature and magnetic shear.

In this work, the measured transport profiles are compared with growth rates obtained from a simple dispersion relation. Following Ref. [8], the parallel ion dynamics may be disregarded to arrive at growth rates

$$\gamma = \frac{\delta c_s \rho_s k_\alpha}{(1 + \rho_s^2 k_\perp^2)^2} \frac{B}{\chi'} \left( (\ln n_0)' - \frac{2}{\sqrt{G^{ss}}} \left( \kappa_n - \kappa_g \frac{\chi'}{B} G^{ss} (\Lambda + \Theta_k) \right) \right) \quad (1)$$

with the magnetic field strength  $B$ , the poloidal flux  $\chi$ , the sound speed  $c_s = \sqrt{T_e/M_i}$ , the drift scale  $\rho_s = \sqrt{T_e M_i}/eB$ ,  $\kappa_n$  the normal and  $\kappa_g$  the geodesic curvature and  $\Lambda = G^{\alpha s}/G^{ss}$  the integrated local magnetic shear (ILMS). The radial coordinate  $s$  is the normalised poloidal flux and  $\alpha = \varphi - q\theta$  the field-line label with metric coefficients  $G$ . The prime denotes the radial derivative  $d/ds$ . The perpendicular wavenumber  $k_\perp$  is expressed in terms of  $k_\alpha$  and  $k_s$  with the ratio  $\Theta_k = k_s/k_\alpha$ . The second term in the brackets of Eq. (1), which arises from the compressibility of  $\tilde{\mathbf{v}}_{E \times B}$ , contains the relevant geometry dependent components and will be discussed next.

**Comparison of turbulent transport and linear growth rates:** From Eq. (1) it can be seen that negative normal curvature contributes to a destabilisation of drift modes. The geodesic curvature basically shows up in the product with the ILMS if the radial structure of the fluctuations is neglected ( $k_s = 0$ ). For TJ-K, the geometrical quantities were calculated by means of a field-line tracing code. Metric coefficients were calculated from neighbouring flux surfaces in Boozer coordinates and mapped back into the laboratory frame of reference. In Fig. 2,  $\kappa_n$ ,  $\kappa_g$  and the ILMS are shown as contour plots in the triangular cross-section. The normal curvature shows

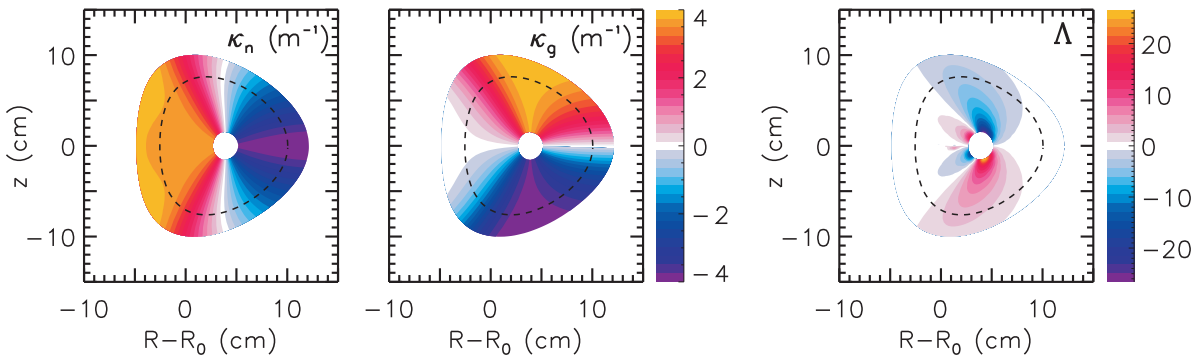


Fig. 2: Contour plots of the normal (left) and geodesic curvature (centre) as well as the ILMS (right) in the triangular poloidal cross section. The dashed line marks the position of the poloidal probe array.

an in/out asymmetry with negative values on the outboard side (here LFS) and the geodesic curvature an up/down asymmetry with positive values in the top half. Regarding the growth rate, however, the asymmetry in  $\kappa_g$  is compensated in the product with  $\Lambda$ , which is also up/down asymmetric. The only ingredient, which in the present case could formally break the up/down symmetry as observed in the measured transport profile, is a finite radial wavenumber ( $k_s \neq 0$ ).

For a direct comparison with the transport profile, the curvature dependent part of  $\gamma$  is computed with  $\Theta_k = 1$  and, everywhere,  $\rho_s k_\perp = 1$ , which locally sets  $k_\alpha$  to yield the maximum possible growth rates. The result is shown in Fig. 3. With  $\Theta_k > 0$  the maximum growth rate is shifted into the direction of the ion-diamagnetic drift and in comparison, the region with  $\gamma > 0$  coincides with the region of maximum turbulent transport. Poloidal transport profiles have also been measured at another toroidal position with different magnetic field topology [2]. Here, a good agreement in the localisation of maximum transport and calculated growth rates is found, too.

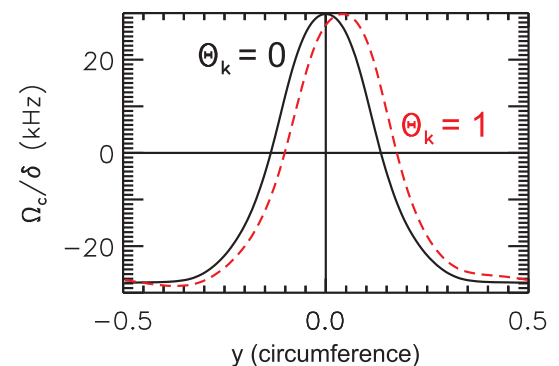


Fig. 3: Curvature dependent part of  $\gamma$  calculated at the position of the poloidal probe array.

**Summary:** Linear drift-wave growth rates from a simple dispersion relation [8] were calculated for the magnetic field topology in the stellarator TJ-K and compared to turbulent transport measurements on the full circumference of a flux surface in the poloidal cross section. A good agreement in the localisation of maximum transport and calculated growth rates was obtained. A poloidal shift of the maximum growth rates away from the symmetry point could be related to the radial structure of the potential fluctuations. Finite radial wavenumbers are accompanied by poloidal  $E \times B$  drifts. Those are associated with compression due to  $B$  variations on the flux surface, of which the geodesic curvature is a measure. Thus, maximum growth rates are shifted towards positive geodesic curvature.

The model does not take into account the experimental fact that the density-potential cross-phase is subject to spatial variations. The maximum growth rates presented here base on the assumption of a constant delay. Moreover, they are not specific to particular modes. They may rather be regarded as an indicator of local curvature drive capabilities in the underlying magnetic field configuration. The local drive could be reflected in the spatial dependency of the cross phase and, thus, in the turbulent transport, which is supported by the observed agreement of growth rate and transport maxima.

## References

- [1] U. Stroth *et al.*, Phys. Plasmas **11**, 2558 (2004).
- [2] G. Birkenmeier *et al.*, Phys. Rev. Lett. (2011), accepted.
- [3] M. Ramisch *et al.*, *Proc. of the 35<sup>th</sup> EPS Conf. on Plasma Phys., Hersonissos, Crete* (2008), Vol. 32D, pp. P-4.028.
- [4] A. Bhattacharjee *et al.*, Phys. Fluids **26**, 880 (1983).
- [5] R. E. Waltz and A. H. Boozer, Phys. Fluids, B **5**, 2201 (1993).
- [6] A. Kendl and H. Wobig, Phys. Plasmas **6**, 4714 (1999).
- [7] M. Nadeem, T. Rafiq, and M. Persson, Phys. Plasmas **8**, 4375 (2001).
- [8] M. H. Nasim, T. Rafiq, and M. Persson, Plasma Phys. Control. Fusion **46**, 193 (2004).